ISSN: 2640-5571

Research Article

Advances in Nanoscience and Nanotechnology

# Photo-Thermal Catalytic Reduction of Carbon Dioxide: Recent Status and Future Prospects

**Sushil Kumar, Sk Riyajuddin, Gushandeep Kaur, Kaushik Ghosh***

*Institute of Nano Science & Technology, Knowledge City, Sector-81, SAS Nagar, Mohali-140306, India.*

***Corresponding author**
Kaushik Ghosh, Institute of Nano Science & Technology, Knowledge City, Sector-81, SAS Nagar, Mohali-140306, India.

**Submitted:** 30 Jun 2020; **Accepted**:31 July 2020; **Published**: 26 Jun 2021

***Citation:*** *Sushil Kumar, Sk Riyajuddin, Gushandeep Kaur, Kaushik Ghosh (2021) Photo-Thermal Catalytic Reduction of Carbon Dioxide: Recent Status and Future Prospects. Adv Nanoscie Nanotec 5(1): 5-19.*

## Abstract

*Enormous emissions of carbon dioxide (a greenhouse gas) produced from burning of fossil fuels, industrial revolution and rapid urbanisation originate the greenhouse effect and also ocean acidification, thereby posing a great threat to entire environment. Massive efforts have been devoted to transform carbon dioxide into useful products for sustainable development in the sectors of energy as well as environment. However, efficiently reducing the carbon dioxide is highly challenging due to higher thermodynamic stability of carbon dioxide. Among the several potentials routes possible, carbon dioxide conversion by coupling the photo and thermal energy is particularly attractive as abundant solar energy can be utilised. In this review, we provide a comprehensive overview of photo thermal carbon dioxide reduction and summarized the recent developments and clear understanding of hydrogenation of carbon dioxide by coupling the photo and thermal energy. Firstly, basic principle of coupling of solar and thermal energy is elaborated and further, discussed the current status and future challenges of implementing this strategy for carbon dioxide transformation. Ultimately, the outlook to future for reduction of carbon dioxide via coupling of photo and thermal energy is discussed.*

**Keywords:** $Co_2$ Reduction, Coupling of Photo and Thermal Energy, Lspr Effect, Nanostructures.

## Introduction

The rapid urbanization during last two decades and the industrial revolution, since the 1860s, lead to an exponential rise in anthropogenic (or industrial) carbon dioxide emission, a nonvisible greenhouse gas [1]. During year 1958 to 2018, a huge jump in the atmospheric carbon dioxide levels is noticed from 315-410 ppm (Figure 1) [2]. The enormous emission of carbon dioxide ($CO_2$), can bring on the greenhouse effect, result in origin of global warming and melting of glaciers and then, causing an increase in sea level and eventually posing a great threat to environment [3]. The global warming origin with the leap up in anthropogenic greenhouse gas amount is verified by the Intergovernmental Panel on Climate Change (IPCC) 5th Assessment Report (AR5) issued in 2013-14 [4]. Additionally, the same IPCC report (AR5) specifies that to prevent the climate change, it is indispensable to make the temperature increase less than 2° C comparative to preindustrial level and the carbon dioxide concentration should be lowered down worldwide by 41–72% by 2050 and by 78–118% by 2100 relative to 2010 levels. Further, the huge amounts of carbon dioxide produced from fossil fuel incineration and deforestation is soaked by the sea surface which causes a dip in pH and alters seawater carbonate chemistry and finally, extensively affecting marine organisms [5, 6].

To address the issue of global warming adequate efforts, need to be taken, ranging from private homes to large industry scale. Driving and flying less, using less energy consuming appliances and recycling etc. are the person level initiatives can check the "carbon footprint". To curb this issue fully, government is also actively taking measurements. However, all these efforts can aid to control pollution, they are not capable of tackling with the matter arising from the rapid urbanization [1]. The most promising method to curb this problem is conversion of carbon dioxide to clean fuel to simultaneously reduce the global warning issue and fossil fuel consumption and, is emerging as an excellent technique for sustainable progress in the energy and environmental sectors [7, 8]. $CO_2$ can be utilised as a C1 feed stock for the synthesising value-added chemicals/fuels including hydrocarbons, syngas, alcohol, acids carbonates, carbamates [9-33].

Carbon dioxide molecule is highly stable, linear having D∞h point group [34]. $CO_2$ activation step includes adding a single electron and then, a radical anion forms. The repulsion among the two electron lone pairs present on the atoms of oxygen and the unpaired

electron on the carbon atom distorts the linear D∞h geometry and the distorted geometry (bent geometry with elongated C-O bond) have an enthalpy of formation -1604KJmol$^{-1}$ which is 0.5eV greater than linear geometry of carbon dioxide [35]. Therefore, the negative adiabatic electron affinity of $CO_2$ makes the addition of single electron highly endothermic [34]. Additionally, in Carbon dioxide the bond dissociation enthalpy of C=O is approximately 750KJmol$^{-1}$, greater relative to many chemical bonds such as C-C (approx. 336KJmol$^{-1}$) and C-H (approx. 430KJmol$^{-1}$) bonds [36]. A high activation barrier is required to overcome the carbon dioxide conversion. Thereby, conversion of carbon dioxide is a huge challenge due to its kinetic inertness and thermodynamic stability [36]. Thermochemical, photochemical and electrochemical pathways generally are employed for conversion of $CO_2$ value added fuels as shown in figure 2 [1, 11, 37-44].

Moreover, particular amount of energy and appropriate catalyst are essential for performing the reduction process of $CO_2$. The catalyst choice depends on the strategy employed for the reducing the Carbon dioxide. For instance, the catalyst should be capable of reducing $H_2$, a side reaction in electrochemical process, in thermochemical process catalyst should be stable at elevated temperature and an appropriate photocatalyst with minimum band gap 1.23eV is required for photochemical method [1].

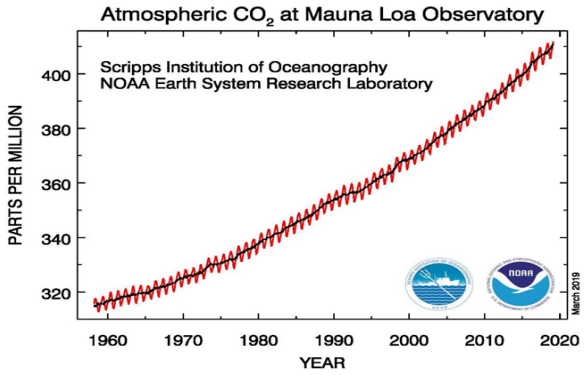


**Figure 1:** Atmospheric $CO_2$ concentration during 1958 – 2018. Adapted from Ref. [2].

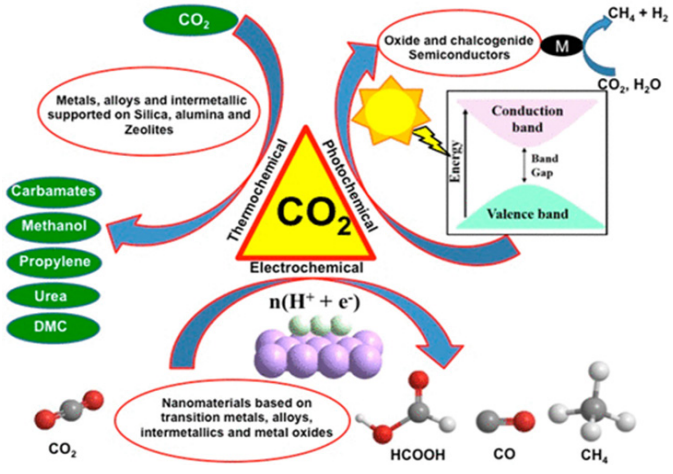


**Figure 2:** Different methods employed for the $CO_2$ to various products. Reproduced from Ref. [1] with permission. Copyright 2018, ACS Publishing Group.

Hydrogenating carbon dioxide electrocatalytically, is emerged as a great technique for carbon dioxide conversion into valuable chemicals and fuels for sustainable carbon cycles [45]. Further, electrochemical carbon dioxide reduction promotes a sustainable low temperature redox cycle for energy storage and conversion. The electrochemical carbon dioxide conversion involves a multiple proton−electron reaction resulting variety of products "P" and water [46].

$$kCO_2 + n\,(H^+ + e^-) \leftrightharpoons P + H_2O$$

where P is the product in aqueous medium (Carbon monoxide, Formic acid, Formaldehyde, Methanol, Methane, Ethanol, Ethylene) and the equilibrium redox potential values are shown in table (1) [47]. The values of redox potential have demonstrated that the redox product nature strongly influence its thermodynamic accessibility from carbon dioxide. The number of electrons engaged in reduction process are important and as the reaction involves multielectron pathways the redox potential becomes more and more negative [48]. The carbon dioxide reduction kinetics is really unfavourable because the first electron transfers to produce CO2•− anion radical after its chemical absorption on the working electrode requires -1.90 V to convert the originally linear molecule into a bent anion radical [47]. Thereby, an appropriate electrocatalyst is required for the activation and reduction of carbon dioxide which can participate in an electron transfer phenomena and increases the rate of a chemical reaction as shown in figure 3. The redox potentials, electron transfer rate and chemical kinetics, current efficiencies are the parameters which evaluate an electrocatalyst [49]. The advantageous approach of electrocatalytic reduction of carbon dioxide is that it can performed at room temperature water can be used as proton source and the chemical utilisation is low making recycling of supporting electrolyte possible [48-51].

However, an inappropriate adsorption energies of key reaction intermediates and the multiple number of proton-coupled electron transfer steps offers chief hurdle of high overpotentials and poor product selectivities for conversion of carbon dioxide. What is more, the competitive evolution of hydrogen reaction, occurring in the exact same range of potentials as carbon dioxide reduction makes the faradaic efficiency really low [46].

Photocatalytic transformation of Carbon Dioxide has been considered an important route to recycle carbon dioxide back to renewable energy with the aid of solar energy, which is considered as one of the best techniques to curb the energy and environmental crises Photocatalytic $CO_2$ reduction (Figure 4) on a semiconductor photocatalyst occurs via five consecutive steps- light absorptions, charge separation, $CO_2$ adsorption, surface redox reaction, and product desorption [52-54]. Upon irradiation with the incident light, the photocatalyst absorbs photons which produces electron and hole pairs and electrons excitations from valance band to conduction band, an equal number of holes leaving in valance band [47]. These charge carriers may drift to the photocatalyst surface and ultimately relocated to the adsorbed acceptor molecules, consequently, the corresponding reduction or oxidation process initiate. Either the semiconductor surface or the interface at the of another semiconductor surface or metal nanoparticle, referred as the co-catalyst may act as the actual reaction site [55]. The pho-

tocatalysts should have optimum band structure for energetically favourable photogenerated electrons or holes for carbon dioxide reduction or water oxidation. For carbon dioxide reduction, the edge of conduction band should be more negative in comparison to redox potential of carbon dioxide hydrogenation and the edge of the valance band must be more positive in comparison to the redox potential of water oxidation (0.817 V vs SHE in pH 7.0 aqueous solution). The band gap should be large enough to consider the associated large over potentials with these electrochemical reactions. However, the solar spectrum utilisation effectively would be limited due to too large band gap of the photocatalysts. Based on these two arguments, 1.8–2.0 eV is estimated as the ideal band gap [47]. The band gap falls off the ideal range for majority of the photocatalysts. Though the integral assembling construction for the light harvester, the charge carrier transferring path, the catalytic sites, and the structural engineering of semiconductor and cocatalyst, have been employed to boost the activity, the low production evolution rate in μmol/h, and even lower performance while employing water as electron donor are still challenging [49]. Fast recombination of excited charge carriers in semiconductors limit the efficiency of photocatalytic process [56, 57]. Kinetic limitations of multiple e/h+ transfer process and limited capability of traditional semiconductors to activate thermodynamically stable $CO_2$ molecules make the photocatalytic carbon dioxide reduction really inefficient [34]. To exemplify, Zhu, S. et al. explored SnNb2O6 nanosheets to perform photocatalytic conversion of carbon dioxide and the maximum methane evolution rate is approximately 4.9μmolg-1 [58].

Thermocatalytic conversion, an alternative route which integrates high temperatures use and with a heterogeneous catalyst to give fast reaction rates and, thereby assisting for large volume production. Thermocatalytic approach can convert carbon dioxide into various synthetic fuels and chemical [30]. Thermodynamics of CO2 reaction is shown below:

$CO_2 + CH_4 \leftrightarrows 2CO + 2H_2$ $\quad \Delta H^\circ_{298K} = +247.3$ kJ/mol

$CO_2 + H_2 \leftrightarrows CO + H_2O$ $\quad \Delta H^\circ_{298K} = +41.2$ kJ/mol

$CO_2 + 4H_2 \leftrightarrows CH_4 + 2H_2O$ $\quad \Delta H^\circ_{298K} = -164.9$ kJ/mol

$CO_2 + 3H_2 \leftrightarrows CH_3OH + H_2O$ $\quad \Delta H^\circ_{298K} = -49.2$kJ/mol

Source of hydrogen is essential for thermocatalytic reduction of carbon dioxide which can be generated via water electrolysis using renewable electricity (solar, wind, or hydro) or using the off-peak, surplus electricity, or low carbon footprint electricity (nuclear power) under appropriate conditions [59]. A thermocatalytic reaction generally involves reactant molecule adsorption over the catalyst surface, intermediate formation and conversion to products and ultimately, product molecule desorption [59, 60]. This process involves transformation of energy and thermal energy (E = kT, where k is the Boltzmann's constant and T the temperature) provides the energy of activation for the progress of reaction [61]. The major drawback of thermocatalytic reduction of carbon dioxide is that the input energy is usually provided by incineration of fossil fuel in an engine [50]. Generally, fixed bed (packed bed) reactors and fluidized bed reactors are employed for thermocatalytic process. Though the Fixed beds are close- fluidized bed reactors packed and easy to run, the heat transfer in packed beds is highly inefficient. On the other hand, fluidized bed reactors provide better transport characteristics. But, fluidized bed reactor is bulky and restricted to a narrow window of operation in terms of flow rates. Therefore, reactor designing is really challenging in thermocatalytic process, particularly thermal management [59]. Furthermore, in thermocatalytic carbon dioxide hydrogenation more attention has been paid to methanation using dry biomass or coal as carbon source making the whole system extremely inefficient due to multiple steps of gasification and separation prior to methanation [62]. Apart from this, the high temperature leads to the migration of nanoparticles of the metal on the surface and interact with each other causing loss of the catalytically active surface area (Sintering) [63]. Although thermochemical conversion of carbon dioxide is a promising technique, extremely high temperature approx. 2000°C and special reactor designing is required to carry out this process [64].

Another important strategy is synergistically combining photo catalytic and thermo catalytic way to boost the endogenic carbon dioxide conversion reaction via the thermal energy produced by plasma photoexcitation from the or black powder samples or noble metal photocatalyst [65]. Recent studies revealed that the solar and thermal energy coupling can significantly enhance the carbon dioxide conversion process with catalytic activities more than the sum of individual photocatalytic and thermo catalytic transformation of carbon dioxide, which offers an entirely new way for carbon dioxide conversion by utilising abundant solar energy [66]. Firstly, the principles of photo thermal conversion of carbon dioxide will be discussed, then the recent developments in photothermal catalytic process and finally, the future challenges and perspectives.

**Table 1: Standard electrochemical potentials for CO2 reduction. Adapted with permission from Ref. [46]. Copyright 2017, Wiley-VCH.**

| Reduction Potential of Car | E° [V] vs SHE at pH 7 |
|---|---|
| $CO_2 + e^- \rightarrow CO_2^-$ | -1.9 |
| $CO_2 + 2H^+ + 2e^- \rightarrow HCOOH$ | -0.61 |
| $CO_2 + 2H^+ + 2e^- \rightarrow CO + H_2O$ | -0.52 |
| $2CO_2 + 12H^+ + 12e^- \rightarrow C_2H_4 + 4H_2O$ | -0.34 |
| $CO_2 + 4H^+ + 4e^- \rightarrow HCHO + H_2O$ | -0.51 |
| $CO_2 + 6H^+ + 6e^- \rightarrow CH_3OH + H_2O$ | -0.38 |
| $CO_2 + 8H^+ + 8e^- \rightarrow CH_4 + H_2O$ | -0.24 |
| $2H^+ + 2e^- \rightarrow H2$ | -0.42 |

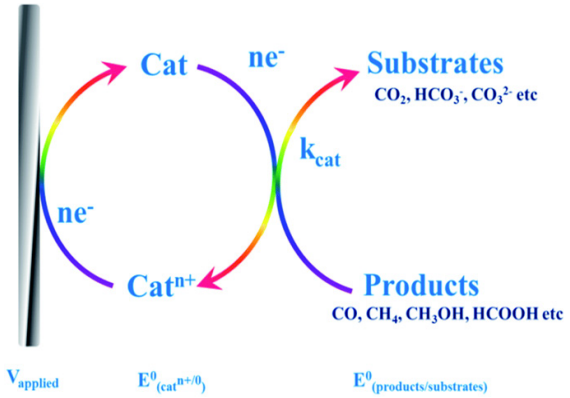


**Figure 3:** Electrocatalysis of $CO_2$ reduction with catalyst loaded on electrode. Adapted from Ref. with permission. Copyright 2013, RSC Publications [48].

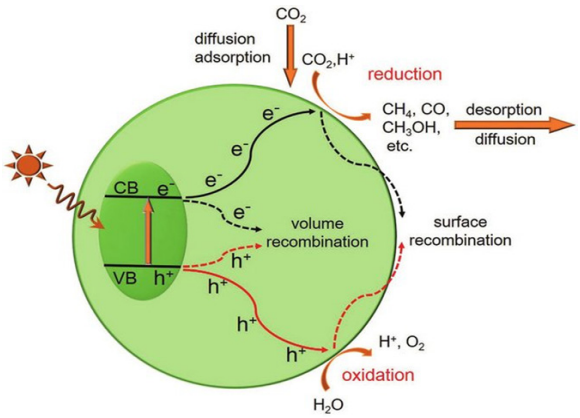


**Figure 4:** Schematic showing the five fundamental steps in photocatalytic CO2 reduction. Reproduced from Ref. with permission. Copyright 2017, Wiley-VCH [46].

Basic Principal of Coupling of Photo and Thermal Energy

The Coupling of photo and thermal energy route for reduction of carbon dioxide has been emerged as the most fascinating route as it enables the utilisation of sustainable energy sources and attain effective catalytic conversion. This technique can be realised via two ways: one is traditional concept of solar thermal heating and the second is plasmonic resonance phenomena [67]. Plasmonic resonance process for photo-thermo catalytic process has been explained well in this review article.

When the light wavelengths are longer comparative to the metal nanoparticles size LSPR effect is established [68]. Local Surface Plasmonic Resonance is a resonant collective oscillation of the outer shell electrons of metal nanoparticles, which arises when the natural frequency of surface electrons oscillating against the restoring force of positive nuclei matches the frequency of an incident electromagnetic field [68-70]. LSPR effect enables the nanoparticles to collect the visible light energy, centralize it in the vicinity of the surface of the particles, and eventually convert light energy into the energy of excited charge carriers [68]. The LSPR excitations lead to strong electric fields in the vicinity of the surface of the particles and these immensely high field intensity regions are commonly referred to as plasmonic hotspot [68-71].

Nonradiative decay of the stored energy in the elevated LSPR fields yield plenty of energized charge-carriers (hot electrons and holes) in the metal nanoparticles that can take place via either intraband s-to-s excitations or interband d-to-s excitations [68, 71-73]. Highly energetic charge carriers (electrons or holes, formed by the plasmon decay) transiently populate otherwise unpopulated electronic states (orbitals), present on the adsorbate molecule due to the LSPR interaction with energetically accessible adsorbate orbitals [69]. The entire adsorbate nanoparticle system is evolved to a different potential energy surface which can result in the activation of chemical bonds and chemical transformations [68,69]. It should be emphasized that momentary exchange of electrons between the metal and reactant occur and adsorbate ions survive on metal surfaces tens of femtoseconds before the relaxation, which is sufficient to induce chemical transformation or add on vibrational energy to the reactant leading to the reaction [68]. The charge injection process on excited plasmonic metal nanoparticles can occur through two routes: direct and indirect route as depicted in Figure 5 [68-70]. In the indirect mechanism, the charge carriers are first produced within the metal and later transferred to unoccupied adsorbate orbitals.

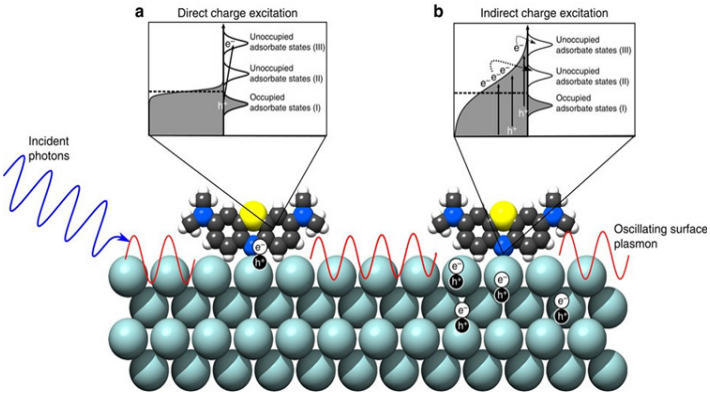


**Figure 5:** Illustration of LSPR-mediated charge excitation mechanisms. Adapted from Ref. with permission [69]. Copyright 2016, Nature Publishing Group.

On the other hand, in direct mechanism an electron is directly excited into an unoccupied adsorbate orbital of matching energy through the decay of an oscillated surface plasmon [69]. In the indirect route, the LSPR enhances the rates of charge excitation and the direct mechanism increases the chemical selectivity.

In photo-thermo catalysis, both photocatalyst and thermocatalyst synergistically take part in the reaction. Coupling of Continuous light of low intensity with thermal energy result photochemical reactions on metallic catalysts at appreciable rates. The plasmonic nanostructures have capability to concentrate the energy of a photon flux efficiently to extremely small volume at their surface and to transfer this energy in the form of energetic electrons to adsorbed molecules [74].

## Recent Prospects in Photo-Thermal Hydrogenation of Carbon Dioxide

In this section, a comprehensive review of various hydrogenation reactions of carbon dioxide through coupling of photo energy and thermal energy is provided.

## Methanation Synthesis

Carbon dioxide reduction to methane also called Sabatier reaction, after the Belgian chemist who investigated the hydrocarbons hydrogenation by employing a nickel catalyst (Sabatier, 1902) [33]. Carbon dioxide methanation is an extremely important process as it arises as a great way to store renewable energy with additional benefit of $CO_2$ emission benefit [67,75]. Carbon dioxide conversion to methane has a wide scale of applications including the and the compressed natural gas formation and including the syngas production [76]. The $CO_2$ methanation reaction has industrial application, provided that renewable sources are used for hydrogen generation [77]. The National Aeronautics and Space Administration (NASA) has carried out research on the methanation of carbon dioxide in manned space colonization on Mars [75]. The conversion of the Martian $CO_2$ atmosphere into methane and water for astronaut life-support systems and fuel is possible [76]. Thermodynamically, carbon dioxide hydrogenation to methane is a highly advantageous reaction, as the reaction is considerably faster comparative to other reactions which give alcohols or hydrocarbons [77].

Although, the $CO_2$ conversion to methane is thermodynamically favourable ($\Delta G_{298K}$ = – 130.8 kJ/mol); reducing the completely oxidized carbon to methane requires eight-electron along with significant kinetic limitations, and hence a catalyst to achieve appreciable rates and selectivities is required [75]. The carbon dioxide methanation has been extensively studied.

$$CO_2 + 4H_2 \leftrightarrows CH_4 + 2H_2O$$
$$\Delta H^\circ_{298K} = -164.9 \text{ kJ/mol}$$

Xianguang Meng et al [64]. employed the Group VIII metals (Ru, Rh, Ni, Co, Pd, Pt, Ir, and Fe) based nanocatalysts over inert Al2O3 support for photothermal catalytic conversion of $CO_2$ with H2 into methane and obtained the CO2 reaction rates six orders of magnitude higher than photocatalytic methods. The catalysts were synthesised by impregnating of mesoporous $Al_2O_3$ (BET surface area=136 $m^2g^{-1}$) in the Group VIII metals precursor solutions, followed by two hours' calcination at 300°C. The carbon dioxide hydrogenation was performed in a batch-type reaction system with molar ration of $H_2/CO_2$ slightly more than 4:1 under irradiation with a 300 W Xenon lamp. The activities and selectivities of all these catalysts for $CO_2$ conversion compiled in table 2 depict that $Ru/Al_2O_3$, $Rh/Al_2O_3$, $Ni/Al_2O_3$, $Pd/Al_2O_3$, $Co/Al_2O_3$ were better than $Fe/Al_2O_3$, $Pt/Al_2O_3$, $Ir/Al_2O_3$. A reaction temperature of 300–400°C was obtained by photoirradiation of group VIII catalysts continuously. Further, by supressing the thermal effect upon irradiating the $Ru/Al_2O_3$ with monochromatic light in visible region the evolution rate of methane was significantly less irrespective of monochromatic light filters which revealed that photo-induced methanation of carbon dioxide over the $Ru/Al_2O_3$ is mediated by a photothermal effect. Authors proposed that effective energy utilization the of the solar spectrum over the wider range, strong photothermal effect, and a unique ability of $H_2$ dissociation (to generate active H atoms, important intermediates for $CO_2$ reduction at low onset temperatures) are various properties of group VIII nanocatalysts responsible for reduction of carbon dioxide efficiently.

Ozin's group synthesised Ru/SiNW catalyst by Ru nanoparticles (10nm) onto black silicon nanowire (100nm diameter) to carry out photo–thermal methanation of gas-phase $CO_2$ in a hydrogen environment in a custom-built stainless-steel batch reactor (1.5 ml) (Figure 6b) [78]. Either resistive heating or solar simulation can be opted for heating the reaction mixture. However, the methanation rate was 5-fold higher under the solar simulation radiation (due to the participation of photons) than resistive heating. On comparing the activity of Ru nanoparticle catalyst over different supports in dark as well as light irradiation under solar simulated light from a Xe lamp at a temperature of 150°C, it was revealed that, methane conversion rates of carbon dioxide were maximum over the Ru/SiNW catalyst (Figure 6a), proceeding at a rate of 0.51 mmol $g^{-1}$ h-1 in the dark and raising by 94% to 0.99 mmol g-1 h-1 in the light. Further experimental results also proved that rate of reaction is maximum at intermediate pressure. Authors proposed that photogenerated electron-hole pairs formed due to absorption of photons by Si NWS which form the active hydrogen atoms on the surface of Ru and finally Ru-H bond formation enhance the overall photo methanation reaction. This work demonstrated that Si NW supported Ru nanoparticles are capable of efficient hydrogenation of $CO_2$ to methane without any source of external heating.

**Table 2: Activities and selectivities of the Group VIII catalysts. [a] Adapted with permission from Ref. [64]. Copyright 2014, Wiley-VCH**

| Sample | Metal loading[b] [wt %] | Rmax[c] [mol $h^{-1}$ $g^{-1}$] | Conversion[d] of $CO_2$ [%] | Selectivity[d] for $CH_4$ [%] | Selectivity[d] for CO [%] |
|---|---|---|---|---|---|
| $Ru/Al_2O_3$ | 2.4 | 18.16 | 95.75 | 99.22 | 0.78 |
| $Rh/Al_2O_3$ | 2.6 | 6.36 | 96.25 | 99.48 | 0.52 |
| $Ni/Al_2O_3$ | 2.1 | 2.30 | 93.25 | 99.04 | 0.95 |
| $Co/Al_2O_3$ | 2.5 | 0.90 | 92.58 | 99.51 | 0.49 |
| $Pd/Al_2O_3$ | 2.0 | 0.53 | 93.43 | 98.64 | 1.36 |
| $Pt/Al_2O_3$ | 2.4 | 0.47 | 60.42 | 15.55 | 84.45 |
| $Ir/Al_2O_3$ | 2.8 | 0.05 | 14.94 | 63.25 | 36.74 |
| $Fe/Al_2O_3$ | 2.4 | 0.02 | 7.27 | 4.04 | 95.96 |
| $TiO_2$ | – | 9.04×10−7 | – | 68.23 | 31.77 |
| $Pt/TiO_2$[e] | 2.5 | 8.01×10−9 | – | 100 | 0 |
| Ru/TiO2[e] | 2.5 | 5.31×10−9 | – | 100 | 0 |

[a] For the reaction conditions, [b] Loading amounts of the Group VIII nanoparticles determined by ICP-OES. [c] Rmax: the maximum $CO_2$ reaction rate. [d] Based on the amount of the gas at the end of the reaction. [e] Water (2 mL) was used instead of H2 as the hydrogen source.

JiaN Ren et al [79]. focused to design a 2D nanostructured catalyst, constructed by ultrathin Mg–Al LDHs matrix and Ru nanoparticles (denoted as Ru@FL-LDHs) (Figure 7) with targeting activation function for $CO_2$ and $H_2$ for the photo-thermal methanation reaction. The catalyst was fabricated by impregnating 1 g of FL-LDHs into 13.2 mL of 4 $gL^{-1}$ $Ru_3(CO)_{12}$/acetone solution with mild stirring, heating the resulting suspension up to 70°C for solvent removal, followed by sintering at 160 °C for 2 h. The photo-thermal methanation reaction was conducted in a flow type reactor (total volume 330mL), employing a 300 W Xe lamp as light source, using 150 mg of catalyst and gas mixtures of carbon dioxide and hydrogens slightly more than 4:1. A maximum yield of 277 mmol $g^{-1}$ $h^{-1}$ (catalyst) for formation of $CH_4$ was reported over Ru@FL-LDHs, which was significantly greater comparative to previous LDH-based catalysts reports (Fig 8a). What is more, the Ru@FL-LDHs catalyst was proved to be highly stable up to the run period of 12h (Fig 8b). Authors proposed, the exfoliation of ultrathin LDHs matrix provided plenty of surface hydroxide groups which enhance the carbon dioxide chemisorption and activation. Additionally, the role of Ru nanoparticles (under light irradiation) is raising the local temperature for $H_2$ activation and ultimately, to initiate the hydrogenation of carbon dioxide.

Dai et al [80]. fabricated a $Ru/TiO_{2-x}N_x$ catalyst by loading Ru on nitrogen doped $TiO_2$ support using impregnation-reduction method. The carbon dioxide methanation was conducted in a fixed bed flow reactor under atmospheric pressure, heating the reaction mixture by an electric resistance board. The reaction performance was remarkedly enhanced with visible light irradiation (435 nm < λ < 465 nm). Experimental analysis has revealed, the photo-assisted effect of visible light over $Ru/TiO_{2-x}N_x$ catalyst originates from two aspects: First and foremost, due to the oxygen vacancies generated over the $Ru/TiO_{2-x}N_x$, the $CO_2$ adsorption and its activation into the CO would be significantly enhanced. Second, transfer to the Ru nanoparticles, surface electron density of Ru would increase as the photo-generated electrons induced by visible light over $Ru/TiO_{2-x}N_x$ can be transferred to Ru nanoparticles and promote the carbon dioxide activation. For photo-thermo processes, the importance of light adsorption by the metal supported substrate is clearly depicted by this work.

Hydrogenation of carbon dioxide using transition metals can occur through two competitive process: reverse water gas shifts and carbon dioxide methanation, giving carbon monoxide and methane as major products respectively. Everitt's and Liu's et al [81]. found that in hydrogenation of carbon dioxide Rh nanoparticles are capable of reducing the activation energy as well as tuning the product selectivity, with light irradiation. The $Rh/Al_2O_3$ was synthesised by dispersion of Rh nano cubes (37nm) on $Al_2O_3$ nanoparticles (Figure 9a) and a fixed-bed reaction chamber with a quartz window was taken to perform the reaction. (Figure 9b). Under dark at 623K the carbon monoxide as well as the methane generation rates were same. However, on illuminating Rh particles with light, the energy of activation was lowered along with enhanced selectivity (about 6 times) towards methane production over carbon monoxide. Density functional theory calculation revealed that the hot electrons (attributed to LSPR phenomena on the plasmonic Rh nanoparticles) injected in the anti-bonding states of the CHO (reaction intermediate) reduces the activation energy and assist the activation of carbon dioxide towards methane (Figure 10). This work highlighted the product selectivity tuning in carbon dioxide hydrogenation by injecting the photo-excited hot electrons in the antibonding orbitals of the key reaction intermediate.

Jingxiang Low et al [82]. fabricated $TiO_2$ photonic crystals ($TiO_2$ PCs) using template-free anodization–calcination route for Photocatalytic carbon dioxide hydrogenation by drawing in-situ heat from surroundings, to rise the activity of photocatalytic process through Localized Surface Photothermal Effect (LSPT effect) of photonic crystal. These $TiO_2$ PCs have capturing ability of specific photon energy/heat radiation The SEM images (Figure 11) of $TiO_2$ PCs revealed that $TiO_2$ PCs have a typical macroporous photonic crystal structure, comprised of periodically arranged air cylinders having 100 nm average diameter. It was examined by authors that due to its slow photon effect and localized surface photothermal (LSPT) effect photocatalytic performance of $TiO_2$ PCs for methane formation is higher compared to commercially available TiO2 and TiO2 nanotube arrays. $TiO_2$ PCs are capable of absorbing heat radiation at range for boosting adsorption of the reactant attributed to LSPT effect and increasing the separation of electron–hole pair. Photocatalytic $CO_2$ reduction performance of $TiO_2$ PCs significantly enhanced due to collaborated LSPT effect and the extraordinary optical properties.

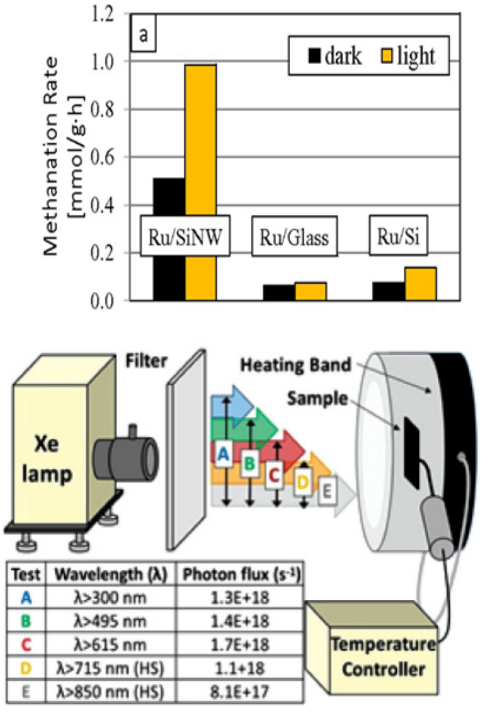


**Figure 6:** Photo-thermo reduction reaction over the Ru/SiNW catalyst (a) Methanation rates over Ru-based catalysts on the SiNW, glass and polished Si supports at 150 °C and 45 psi. b) Schematics of the batch reactor for activity test. Reproduced from Ref. with

permission. Copyright 2014, Wiley-VCH [78].

Li Y synthesised $TiO_{2-x}CoO_x$ by introducing slight oxygen vacancies $TiO_2$ nanotube and

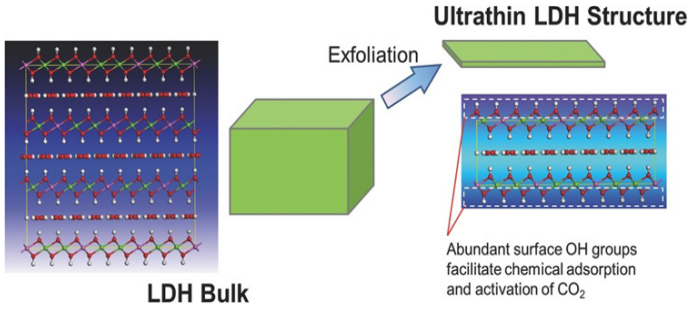


**Figure 7:** Schematic presence of the formation of ultrathin LDH structure with abundant surface hydroxyl groups [83]. Taken from Ref. [79] with permission. Copyright 2016, Wiley-VCH.

Ultralow amount of $CoO_x$ for photo-thermo catalytic reduction CO2. An autoclave with a 100 ml volume was used for Photothermal conversion of $CO_2$. The sealed clave was heated to 393 K irradiated from the top with a 150 W UV lamp and the sample was irradiated with the light intensity of 20 mW/cm$^2$ at 365 nm. Compared with conventional photocatalytic process at 298 K, the yield of $CH_4$ for photothermal reduction under ultraviolet irradiation at high temperature of 393 K was 111.3 times higher on the $TiO_{2-x}$/$CoO_x$ and 175.1 times greater yield of CH4 than the pristine $TiO_2$ under the same photothermocatalytic conditions. Control experiments together with HRTEM, ESR, transient photovoltage measurements demonstrated that the oxygen vacancies facilitate the adsorption and hydrogenation of $CO_2$ and the dispersion of $CoO_x$ nanoclusters and the grafted $CoO_x$ acts as a hole trap to promote more protons release.

Min Xu et al [84]. fabricated the $TiO_2$-graphene ($TiO_2$-G) composite by using a glucose-assisted solvothermal strategy and optimized the graphene content to the formation of strong interfacial interactions for photothermal effect on photo catalytic conversion of $CO_2$. The photocatalytic process was performed in a sealed batch reactor by employing 300W Xe lamp as the light source with an intensity of 4.38 kW m$^{-2}$. The TEM analysis revealed that $TiO_2$ NPs have well-defined edges and corners and after introducing graphene oxide, the $TiO_2$ NPs were uniformly adhered to the graphene layers to the formation of $TiO_2$-G composite. Experimental results revealed that the TiO2-G composite exhibited the highest $CH_4$ evolution rate of 26.7 µmol g-1 h$^{-1}$ and CO evolution rate of 5.2µmol g-1h$^{-1}$ 5.1 and 2.8 times higher than $CH_4$ and CO evolution of pure $TiO_2$. Upon light illumination, as a result of photothermal effect, the introduction of 30 mg of graphene leads to a dramatic increase in the surface temperature of photocatalyst from 58.9 to 116.4°C under light illumination of 4.38 kW m$^{-2}$. It was concluded that the superior photocatalytic performance towards $CO_2$ conversion can be because of the synergetic effect of improving charge separation efficiency and surface temperature of $TiO_2$ photocatalyst.

To summarize, Group VIII metals nanoparticles, Ru/SiNW, Ru@FL-LDHs, $Ru/TiO_{2-x}N_x$, $Rh/Al_2O_3$, $TiO_{2-x}CoO_x$, $TiO_2$-graphene, was employed for photo-thermal methanation of carbon dioxide and increased activity towards methane synthesis was seen.

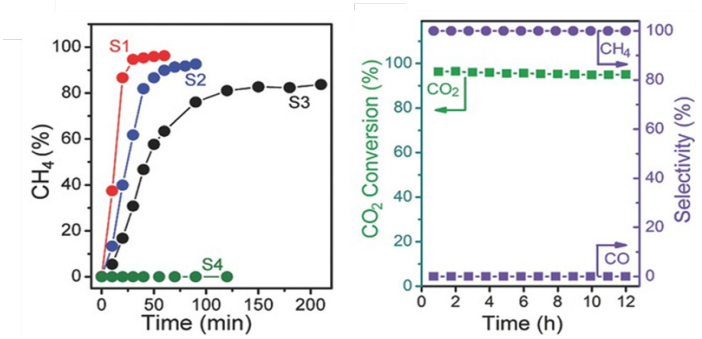


**Figure 8:** a) CH4 product in photothermal conversion of $CO_2$ over Ru loaded catalysts and FLLDHs matrix. b) Long-term test of photothermal $CO_2$ conversion over Ru@FL-LDHs. Reaction condition: 150 mg catalysts, H2: 20.5 mL min-1, $CO_2$: 5.0 mL min-1,300 W Xenon lamp. Samples: S1, Ru@FL-LDHs; S2, Ru@LDHs; S3, Ru@$SiO_2$; S4, FL-LDHs. Reproduced with permission from Ref. [79]. Copyright 2016, Wiley-VCH.

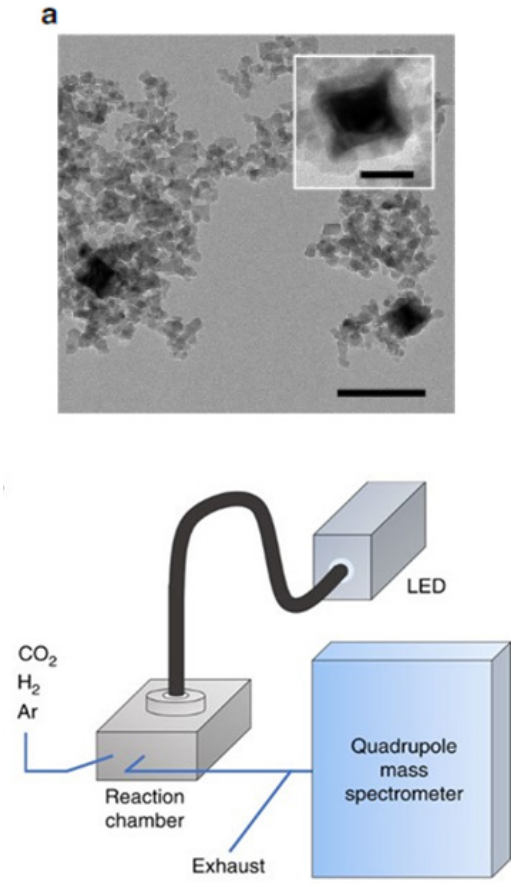


**Figure 9:** a) TEM image of $Rh/Al_2O_3$ photocatalyst. b) Schematic of the photocatalytic reaction system, consisting of a stainless -steel reaction chamber having a quartz window, LEDs coupled through a light guide, and a mass spectrometer for product analysis. Adapted from Ref. [81] with permission. Copyright 2017, Nature Publishing Group.

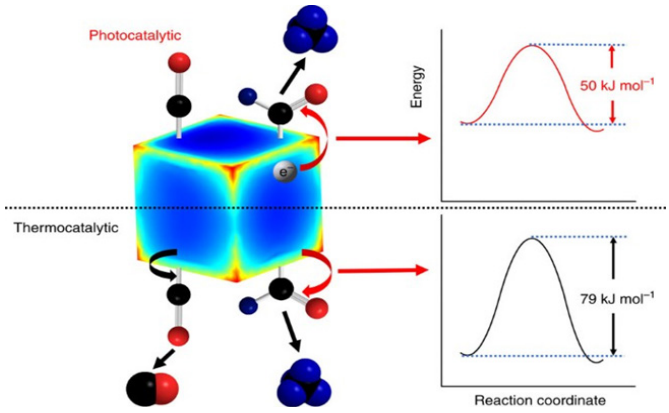


**Figure 10:** Reaction mechanism on a rhodium nanocube. Adapted from Ref. with permission. Copyright 2017, Nature Publishing Group [81].

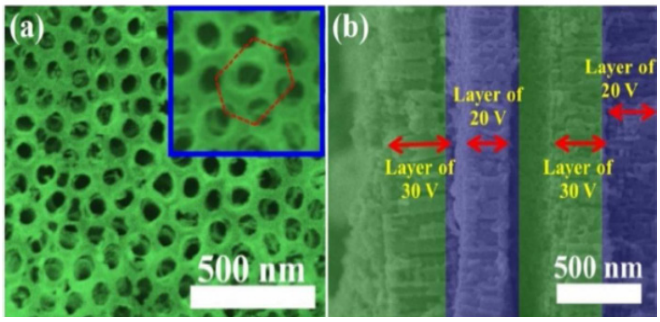


**2.2 Methanol Synthesis and and C2+Product synthesis:** Methanol formation from carbon

**Figure 11:** a,b) Top view (a) and cross-sectional view (b) scanning electron microscope (SEM) images of TiO2 PCs. Reused with permission from Ref [82]. Copyright 2018, ACS Publications.

Dioxide and hydrogen is highly attractive attributed to its great application as a fuel (either pure or by mixing with other fuel) producing less harmful gases, as the starting material for various other beneficial chemicals and a commodity chemical [85-87]. Further, methane formation by Carbon dioxide is an excellent way to regulate the increasing level of atmospheric carbon dioxide and by utilising renewable H2 and carbon dioxide can be incorporated into a carbon cycle [88]. Industrially synthesis of methanol is carried out by using conversion of syngas over a Cu-ZnO/$Al_2O_3$ catalyst at 493−573 K and between 5-10 MPa [89]. Thermodynamically hyrdogenation of carbon dioxide to methanol is favourable at low temperature and elevated pressure. Since the reaction is slow at low temperature kinetically. Carbon dioxide activation occurs with a significant rate only at the temperature greater than 200°C. However, under these circumstances, the methanol selectivity and yield decrease due to the side product (CO, hydrocarbons and alcohols) formation. Thereby, fabrication of catalyst having high methanol selectivity is extremely important [90].

Ozin et al [91]. reported $In2O_{3-x}(OH)_y$ having a rod-like nanocrystal superstructure for methanol synthesis from photo-thermo transformation of carbon dioxide at atmospheric pressure. The reaction was conducted in a flow type reactor at three different temperatures 200°C, 250°C, and 300°C. However, the optimal temperature was 250°C. At 250°C, methanol formation was enhanced to 97.3µmolg-$1h^{-1}$ upon light irradiation with reduced product selectivity. During a 20h measurement, methanol generation rate of 0.064mmol gcat-1h-1 and 50% selectivity was seen which revealed higher photocatalytic stability of $In2O_{3-x}(OH)y$ rod-like nanocrystal superstructures in photo-thermo carbon dioxide conversion to methanol. The excellent photo-thermo performance of $In2O_{3-x}(OH)_y$ was due to nanocrystal superstructures which elongated the photoexcited charge carrier's lifetime. Computational studies revealed the unique reactivity of FLSP sites (Surface Frustrated Lewis Pairs) made by surface hydroxide being near an oxygen vacancy, enhanced the methanol synthesis under light conditions.

Dengdeng Wu et al [92]. designed Pd/ZnO catalyst by the dispersion of Pd onto commercial ZnO for photothermal hydrogenation of $CO_2$ to methanol. The catalyst was fabricated by impregnation method and TEM images analysed that Pd nanoparticles were evenly distributed on ZnO surface (Figure 12a). The photothermal catalytic reduction of carbon dioxide was performed in a continuous-flow fixed-bed reactor at a low pressure of (12 bar). Whilst comparing the catalytic performance with and without light source it was seen that the light irradiation could significantly enhance the $CO_2$ conversion by more than two times over a temperature range from 190°-270°C. The formation of PdZn alloy evidenced at Pd-ZnO interface. Based on literature studies it is believed that Zn atoms migrate gradually from ZnO onto Pd surface upon $H_2$ treatment and formation of bimetallic PdZn phase take place at Pd-ZnO interface due to intermix with Pd atoms. Control experiment using a filter to cut off the wavelength shorter than 420 nm, the yields of methanol and CO over Pd/ZnO still accounted for 93.5% and 90.4% of those under full spectra irradiation, respectively. It was highlighted that the Pd component plays a significant role in the activity promotion via the utilization of a wide range of visible light. Based on experimental results it was proposed that due to LSPR effect hot electrons are produced on Pd surfaces after absorbing the visible light and transferring the hot electrons to the Pd-ZnO interface occur (Figure 12b) where the formation of PdZn bimetallic phase is verified by TEM and XPS analysis. PdZn serves as active sites by injecting electrons to the antibonding orbitals of carbon dioxide and thereby, accelerate the dissociative adsorption of carbon dioxide and finally, boosting the activation of carbon dioxide.

Zhen-Hong Hea, et al [93]. synthesised CoO/Co/$TiO_2$ catalyst by using impregnation, calcination, reduction, and partially oxidising in air for reduction of carbon dioxide to methanol under photothermal conditions in aqueous medium. The photothermal CO2 hydrogenation reaction was tested in an autoclave (100ml) having a quartz window (40mm in diameter and 10mm in thickness) on the top, heating the reactor to 120°C and a 300W Xe lamp was used as light source. The characterisation results demonstrated that CoO/Co/$TiO_2$ was comprised of Co NPs and $TiO_2$, and CoO film having thickness of 5–6nm which was formed through the partial oxidation of Co° on the surface of Co nanoparticles at room temperature. After varying the loadings of Co species on $TiO_2$ from 2-10wt% the methanol activity was increased to 39.6µmolgcat-1h-1 and methane to $3.9\times10^{-2}$µmolgcat$^{-1}$h1 as charge transfer efficiency could be enhanced. Further, the greater activity of meth-

anol generation was obtained by employing the catalyst calcinated at 450°C. Loss in methanol activity and a slight hike in methane generation was noticed by increasing the calcinated temperature above 550°C. It was put forward that the good catalytic performances were originated from the unique Z scheme structure of catalyst in which Co° species transferred the photo excited electrons to the valance band of CoO and finally converting carbon dioxide to methanol by the electrons accumulated on the conduction band of CoO.

Further, G. Chen et al, synthesised CoFe-based catalysts (denoted as CoFe-x) by directly reducing CoFeAl-LDH nanosheets with $H_2$ at temperatures (x) between 300 and 700 °C and carried out reduction of CO2 under simulated solar excitation [94]. Tuning of product selectivity of reduction of $CO_2$ from CO to CH4 and ultimately high-value C2+ hydrocarbons was observed by altering the surface chemistry of the CoFe-x catalysts by reduction of the precursor of LDH from 300 to 700 °C (Figure 13) in an $H_2$/Ar (10/90, v/v) atmosphere. A CO2 conversion of 78.6%, with selectivity to C2+ of 35.26% was obtained by irradiating the CoFe-650 catalyst with UV-vis light. Density functional theory demonstrated that CoFe-650 catalyst comprised of alumina-supported CoFe alloy nanoparticles which play significant contribution to promote the C-C coupling selectivity. This work explored an entirely new catalytic system for obtaining value added chemicals from conversion of CO2 by utilising abundant solar energy.

Li P et. al, employed Ultrathin Porous AuCu/g-$C_3N_4$ nanocomposite for photothermal catalytic conversion of carbon dioxide. The catalyst was synthesised by using seed crystal mediated method [65]. The catalytic reaction was tested by irradiating the reaction mixture with 300 W Xe lamp ($\lambda > 420$ nm) through a window in the reactor vessel for simulating sunlight illumination and the photocatalytic reaction continued for 5h with varying loading amounts of AuCu alloy. The yield and selectivity of ethanol decreased when the AuCu alloy loading exceeded 1.0 wt% as the excessive AuCu NPs result in increasing agglomeration, which would lessen the number of exposed active sites on the catalyst surface. The reaction temperature was adjusted from 80°-160°C in increments of 20°C. Due to synergistic effect between photonic energy and thermal energy in AuCu/g-$C_3N_4$ catalyst exhibited the highest amount of $CO_2$ reduction, which is 5.6 and 3.9 times in contrast with that of thermal catalysis and photocatalysis, respectively. Additionally, AuCu/g-$C_3N_4$ nanocomposite processes the very high ethanol selectivity of 93.1%, which was considerably higher than that of the Cu/g-$C_3N_4$ and Au/g-$C_3N_4$ nanocomposite catalysts by factors of 2.9 and 6.2, respectively. Based on experimental observations, the authors suggested the migration of photo-generated electrons from g-$C_3N_4$ to AuCu under light illumination leads to higher negative charges on AuCu alloy nanoparticles which enhanced the $CO_2$ adsorption and activation on catalytic surface forming more reaction intermediates and boosting the conversion of CO2 to ethanol.

In summary, $In_2O_{3-x}$(OH)y fabricated by Ozin's group synthesized methanol with appreciable amount, however product selectivity was compromised. Pd/ZnO was reported to synthesis the methanol in which LSPR effect was playing major role. Again, though the methanol yield was increased by 1.5~3 times at 190-250° C, methanol selectivity was lowered. Zhen-Hong Hea, et al. developed CoO/Co/$TiO_2$ catalyst with improved conversion efficiency of carbon dioxide to methanol under photothermal conditions from the Z-scheme structure of the catalyst. It may be noted as although methanol is highly valuable product, only few efforts lead to reduction of carbon dioxide to methanol efficiently. So, more efficient, selective and active catalyst is essential for production from carbon dioxide. Further, carbon dioxide conversion to valuable C2+ hydrocarbons is still highly challenging. Very few works have been detected for photothermal catalytic conversion of $CO_2$ to C2+ hydrocarbons.

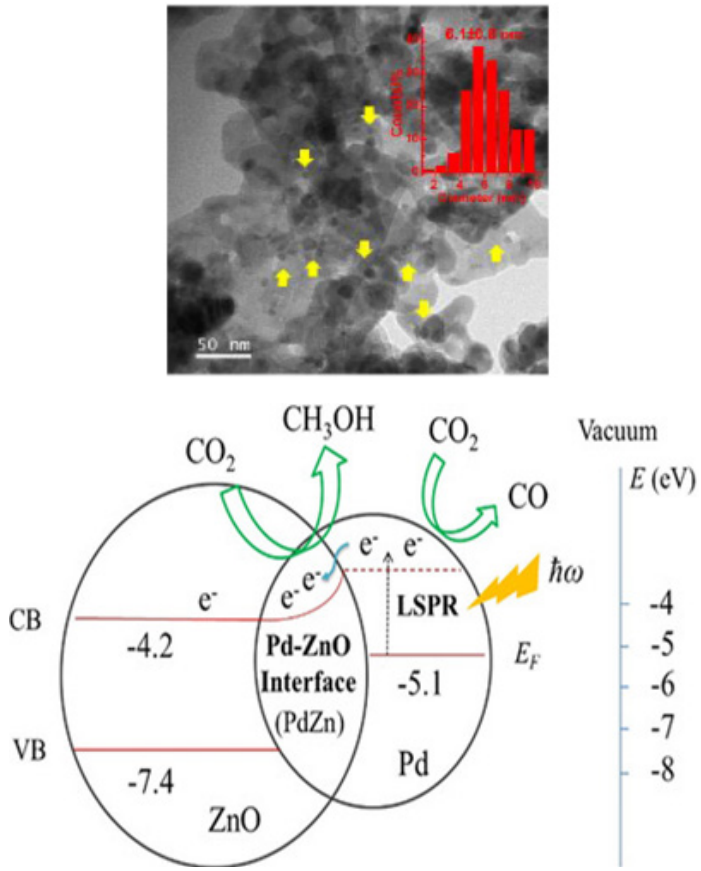


**Figure 12:** a) TEM image and Pd size distribution. b) Mechanism for the photo-induced promotion in CO2 hydrogenation to methanol. Adapted from Ref. with permission. Copyright 2019, Wiley-VCH [92].

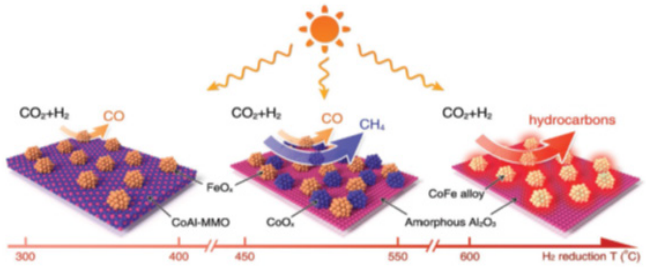


**Figure 13:** Illustration of the different CoFe-x catalysts formed by hydrogen reduction of a CoFeAl-LDH nanosheet precursor at different temperatures. The $CO_2$ hydrogenation selectivity of each CoFe-x catalyst is indicated. Reused from Ref. [94] with permission. Copyright 2017, Wiley-VCH.

## Reverse Water Gas Shift

Carbon Dioxide hydrogenation by reverse water–gas shift reaction is an important catalytic reaction. CO generated by hydrogenation of Carbon dioxide generates methanol or other liquid hydrocarbons by Fischer−Tropsch synthesis [87, 95-97]. Higher concentration of carbon dioxide on Mars and hydrogen availability as a side product of oxygen production offer a commendable opportunity of utilising the RWGS in space exploration [98]. RWGS is a reversible, endothermic reaction ($\Delta H_{298K}$ = 41.2 kJ/mol and $\Delta G_{298K}$ = 28.6 kJ/mol) and is favourable at elevated temperatures [96, 99, 100]. Sometimes, the products removal is essential to shift the reaction equilibrium toward the RWGS rather than the forward Water Gas Shift.99

Wang C. et al [101]. performed Carbon dioxide reduction by plasmonic excitation of ZnO supported Au nanoparticles (designated as Au–ZnO heterostructures) using low power laser illumination (532 nm). SEM image revealed that the Au nanoparticles with diameter 20nm were decorated on ZnO substrate with less particle density (Figure 14a). The CO2 conversion reaction was realised in a gas-tight photocatalysis cell (40ml) fabricated by using a stainless-steel spacer and heating the catalyst to 600°C due to plasmonic resonance excitation. Both methane and CO was detected as the sole products due to the coupling of RWGS and CO methanation. Temperature-calibrated Raman spectra of ZnO phonons demonstrated that product selectivity can by controlled by varying the laser intensity (Figure 14b) which heat the Au–ZnO catalyst in a controlled manner from 30 to 600°C. Product selectivity was tuned from methane to CO by using pulse laser. Though methane was formed at low temperature, there was a continuous hike in generation of CO on increasing the temperature. The experimental observations declared that there was no activity loss of the Au–ZnO catalysts even after repeated illumination with laser and cycling and the solar concentrations was able to attain the light intensity required to start the reaction. This work reported that Carbon dioxide conversion can be executed efficiently by plasmonic resonance effect using visible light and tuning the product selectivity by varying intensity of light.

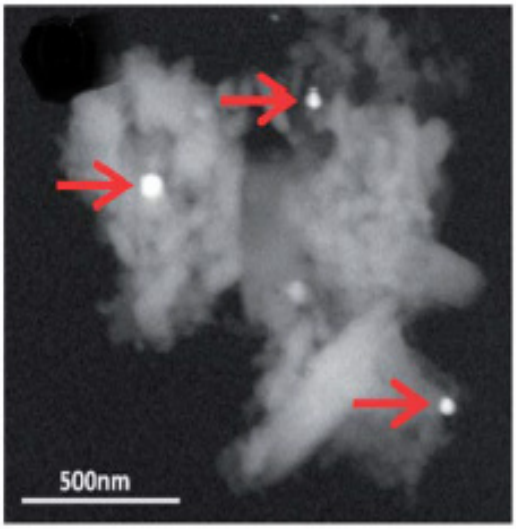


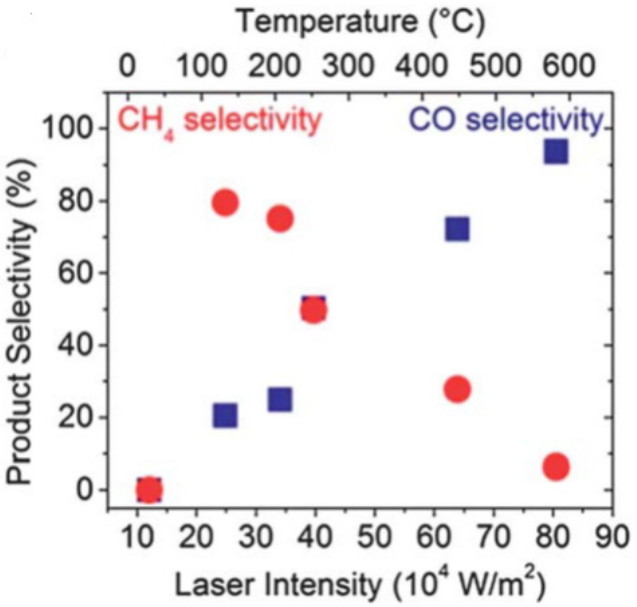


**Figure 14:** a) SEM image of Au-ZnO catalyst. Arrows indicating Au particles. b) Experimental CO (blue squares) and $CH_4$ (red circles) selectivity as a function of cw 532 nm laser intensity and the corresponding catalyst temperature using Au–ZnO catalysts. Reused with permission from Ref. [101]. Copyright 2013, RSC publications.

Aniruddha A [102]. fabricated oxide supported Au catalysts by using deposition-precipitation (DP) method for hydrogenation of $CO_2$ by RWGS reaction and these catalysts are designated as Au/$TiO_2$ (DP), Au/$CeO_2$ (DP), Au/$Al_2O_3$ (DP). The catalytic activities were tested at 400°C and 2:1 molar ratio of $H_2$ and $CO_2$ under visible light illumination and dark conditions. These oxides supported Au catalysts were showing 30 to 130% greater activity for RWGS under light illumination than without light illumination. Out of all the catalysts, Au/$TiO_2$ (DP) displayed maximum conversion rate of 2663µmol/gm-cat/min with light illumination and 2033µmol/gm-cat/min without light illumination and was tested further. Kinetics results revealed that the energy of activation was altered from 47 kJ/mol in dark to 35 kJ/mol in light and apparent order of reaction with respect to $CO_2$ was shifted from 0.5 in dark to 1.0 with light illumination due to the LSPR. Authors stated that the surface plasmons altered the reaction energies either by adjusting the transition state of the rate determining steps or by modifying the adsorption enthalpies of various reactants or intermediates.

Halas's group103 Employed Al@$Cu_2O$ antenna-reactor nanoparticles for effective and selective conversion of carbon dioxide by RWGS under mild illumination at low operating temperature. The catalytic reduction was tested in a flow fixed-bed reactor having a quartz window for visible light illumination. A photon flux of 10$Wcm^{-2}$ on Al@$Cu_2O$ nanoparticles a maximum Carbon monoxide formation rate of 360µmole cm-$2h^{-1}$ and an external quantum efficiency of 0.3% was obtained, which was greater than the previously reported conversions of carbon dioxide. It was seen that the antenna-reactor geometry of Al@$Cu_2O$ nanoparticles enhanced the surface reactivity and the generation of charge carriers in the metal oxide shell. Both the experimental as well as theoretical studies

confirmed that the plasmon-induced carrier generation mechanism was assisting the RWGS. The hot carriers were produced through LSPR damping in Al with immediate transfer to $Cu_2O$ attributed to the line-up of the energy band between aluminium and Cuprous oxide (Figure 15(a, b)). Further, these hot carriers were transferred into the unoccupied orbitals of adsorbed carbon dioxide on the surface of $Cu_2O$ which directly assisted the dissociation of C–O bond and promoted the RWGS reaction. This work highlighted the use of a catalytic system derived from an earth-abundant material rather than precious metals for generation of charge carriers to covert $CO_2$ into CO under mild illumination at low operating temperature.

Li Wang et al [104]. fabricated $CuS/TiO_2$ composites for photo-thermal catalytic $CO_2$ conversion to CO. The $CO_2$ reduction experiments was performed in a sealed reactor at room temperature by irradiating the reactor vertically with a 300W xenon lamp. The XRD studies of $TiO_2$, CuS and 2% $CuS/TiO_2$ composites revealed that CuS and $TiO_2$ have hexagonal and tetragonal structures and there was no change in the crystallographic information of $TiO_2$ after loading CuS. Comparing the UV–Vis–IR irradiation over $TiO_2$, CuS and different ratios of $CuS/TiO_2$, the yield of CO was highest (25.97µmol $g^{-1}$ h-1) over 2% $CuS/TiO_2$. Further experimental results demonstrated that CO yield over 2% $CuS/TiO_2$ under UV-Visible irradiation was 8.53µmol $g^{-1}$ $h^{-1}$ whereas under full spectrum irradiation the CO yield was 25.97µmol g-1 $h^{-1}$ (3 times than the sum value (7.39µmol g-1h-1) of $TiO_2$ (3.39µmol $g^{-1}$ $h^{-1}$ ) and CuS (4.00µmol $g^{-1}$ $h^{-1}$ ). Additionally, the surface temperature of the 2% $CuS/TiO_2$ was reached to 99°C under UV-Visible irradiation and 138°C under full spectrum irradiation. Solar induced photo-thermal synergistic effect enhanced activity of $CuS/TiO_2$ as indicated by the relationship between temperature and photocatalytic activity. CuS is capable of absorbing high quantities of infrared light and its heat conversion and improving efficiency of utilisation of infrared light.

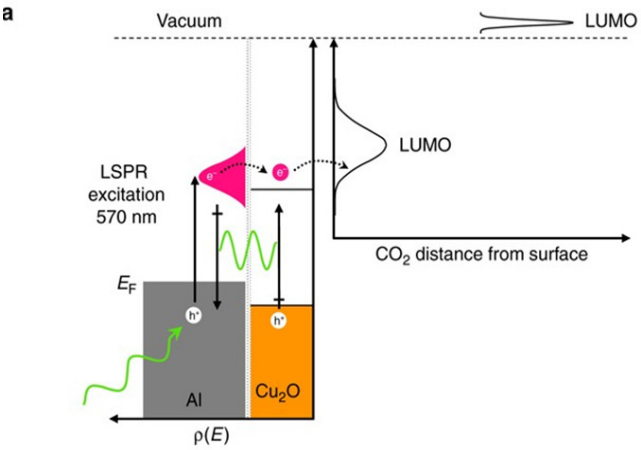


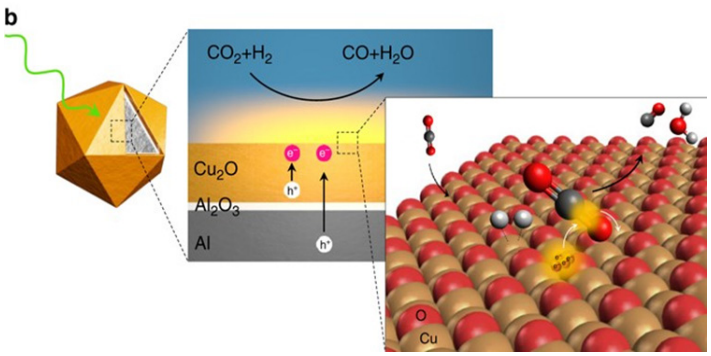


**Figure 15(a, b):** Structure and mechanism of plasmon-induced carrier-assisted RWGS on $Al@Cu_2O$. Reused from Ref. [103] with permission. Copyright 2017, Springer Nature.

B. Lu, et al [105]. constructed a robust catalyst based on Au nanoparticles with $CeO_2$ nanorods (denoted as $Au/CeO_2$) for photothermal reduction of carbon dioxide. The TEM image revealed that the catalyst consists of nanorods (~ 100nm in length) being covered by fine nanoparticles (~ 15nm in size). It was evaluated that the value of band gap for $Au/CeO_2$ (2.5eV) was smaller than that for $CeO_2$ (3.2eV), indicating $Au/CeO_2$ possessed good visible-light absorption. The $CO_2$ hydrogenation was conducted in homemade quartz reactor at atmospheric pressure having a gas mixture (1% $CO_2$, 4% $H_2$, balanced with nitrogen) and was irradiated by a visible light generated from a Xe lamp. For the $CO_2$ hydrogenation, the flow cell was kept on a hotplate (IKA-HS7) to achieve the expected temperature. Experimental results demonstrated that at the same temperature, the $CO_2$ conversion achieved in photothermal process was about 10 times higher than that in thermal process and reached 40% at 400°C. Experimental and theoretical observations proposed that the Au nanoparticles in plasmon resonance have unique ability to absorb photo energy to generate hot electrons, which would efficiently dissociate hydrogen molecule on the catalyst to form Au-H species under photothermal condition. Eventually, the yield of CO would be enhanced as compared to thermal process at same temperature. In summary, Au–ZnO heterostructures, $Al@Cu_2O$ antenna-reactor nanoparticles, $CuS/TiO_2$ composites, $Au/CeO_2$ catalysts were able to enhance the activity in photo-thermo RWGS reactions.

## Challenges and Future Prospect

Undeniably, Photo-Thermal catalytic hydrogenation of Carbon Dioxide is able to make a noteworthy contribution to alleviate exponentially rising levels of carbon dioxide and to overcome the short comings of pre-existing techniques. However, still this catalytic approach is facing plenty of challenges which are needed to be directed in future to make the photo-thermal catalytic technique more reliable.

First, development of photo-thermal catalysis with higher dispersion of supported metal nanoparticles is still challenging. In most of the work presented in photo-thermal catalysis, simple method of impregnation was opted for loading metal nanoparticles on support which causes the irregular distribution of metal nanoparticles. So, in future other methods for dispersion of supported metal nanoparticles are required.

Second, in photo-thermal catalytic carbon dioxide reduction majority of the existing work is related to production of C1 products. However, very limited attention has been given to produce C2+ hydrocarbons like ethanol. Coupling of photo and thermal energy provides a platform to modulate the product selectivity. Thereby, it can serve as a great route to get C2+ hydrocarbons by converting $CO_2$ for future.

Third, catalytic stability is also a matter of huge concern as nanoparticles lose their morphology on exposing to extensive heat. For most of the experiments, the catalytic stability was limited to few hours only. However, to make the photo-thermal catalytic reduction feasible for large scale applications, more attention is required to upgrade the catalytic stability.

Last but not least, hydrogen is the primary requirement for reduction of Carbon dioxide which is not available easily. To implement the photo-catalytic reduction of $CO_2$ at wider scale, renewable source of hydrogen is required. Otherwise, hydrogen production by incineration of fossil fuel will again product $CO_2$. For practical implementation of photo-thermal catalytic reduction of $CO_2$ all the above-mentioned issues should be analysed carefully.

## Summary and Conclusion

Reduction of carbon dioxide via coupling of photo and thermal energy has been proved to be a potential pathway to regulate concentration of atmosphere carbon dioxide as well as to produce value added fuel such as methane, methanol, ethanol, carbon monoxide. Two routes to couple the photo-thermal energy are possible: Surface Plasmonic Resonance where highly intense hotspots are formed due to LSPR effect of plasmonic nanostructures upon exposure to light and the second is traditional solar thermal heating where a light-absorbing material is employed for capturing heat from solar radiations. Clearly, the problems of low efficiency in photocatalytic process and high reaction barriers like high temperature in thermocatalytic can be easily solved via photo-thermal reduction of Carbon dioxide. Selective hydrogenation of Carbon dioxide by photo-thermal technique can also be realised. For example, $Rh/Al2O_3$ was designed to selectively reduce carbon dioxide to methane, selectivity of $In2O_{3-x}(OH)y$ catalyst was modified by carrying out reaction at three different temperatures, CoFe-Al-LDH nanosheets were capable of tuning the product selectivity from CO to methane and finally, to C2+ hydrocarbons. Apart from this, the Coupling of photo and thermal energy has enabled us to perform the reduction of carbon dioxide at ambient conditions that is at moderate temperature and low pressure. To recapitulate, photo-thermal catalytic hydrogenation of carbon dioxide is an excellent way to product value added products.

## Acknowledgment

This work is financially supported by the grant of Nanomission, Department of Science & Technology, India (Grant No: SR/NM/NS-91/2016) and the Institute of Nanoscience & Technology start-up grant.

## References

1. Sebastian C. Peter (2018) Reduction of $CO_2$ to Chemicals and Fuels: A Solution to Global Warming and Energy Crisis. ACS Energy Letters 3: 1557-1561.
2. Pieter T, Keeling R (2012) $Co_2$ Data Mlo.Pdf. Recent Mauna Loa $CO_2$.
3. J Hansen, D Johnson, A Lacis, S Lebedeff, P Lee, et al. (1981) Climate impact of increasing atmospheric carbon dioxide. Science 213: 957-966.
4. RK Pachauri, LA Meyer, Ismail Elgizouli (2014) Climate Change 2014: Synthesis Report. Contribution of Working Groups I, II and III to the Fifth Assessment Report of the Intergovernmental Panel on Climate Change. Intergovernmental Panel On Climate Change 2014: 151.
5. Raven J, Ken Caldeira, Harry Elderfield Frs, Ove Hoegh-Guldberg, Peter Liss, et al. (2005) Ocean acidification due to increasing atmospheric carbon dioxide. Coral Reefs 2005: 68.
6. Scott C Doney, Victoria J Fabry, Richard A Feely, Joan A Kleypas (2009) Ocean Acidification: The Other $CO_2$ Problem . Annual Review of Marine Science 1:169-192.
7. Michele Aresta, Angela Dibenedetto, Antonella Angelini (2014) From $CO_2$ to Chemicals, Materials, and Fuels: The Role of Catalysis. Encyclopedia of Inorganic and Bioinorganic Chemistry 2014:1-18.
8. Soumyabrata Roy, Arjun Cherevotan, Sebastian C Peter (2018) Thermochemical CO2 Hydrogenation to Single Carbon Products: Scientific and Technological Challenges. ACS Energy Letters 3: 1938-1966.
9. Tran Ngoc Huan, Daniel Alves Dalla Corte, Sarah Lamaison, Dilan Karapinar, Lukas Lutz, et al. (2019) Low-cost high-efficiency system for solar-driven conversion of $CO_2$ to hydrocarbons. Proceedings Of The National Academy Of Sciences Of The United States Of America 116: 9735-9740.
10. Gattrell M, Gupta N, Co A (2016) A review of the aqueous electrochemical reduction of $CO_2$ to hydrocarbons at copper. Journal of Electroanalytical Chemistry 594: 1-19.
11. Somnath C Roy, Oomman K Varghese, Paulose M, Grimes CA (2010) Toward Solar Fuels : Photocatalytic Hydrocarbons. ACS Nano 4:1259-1278.
12. Hori Y, Kikuchi K, Murata A, Suzuki S (1986) Production of Methane and Ethylene in Electrochemical Reduction of Carbon Dioxide At Copper Electrode in Aqueous Hydrogencarbonate Solution. Chemistry Letters15: 897-898.
13. David W DeWulf, Tuo Jin, Allen J Bard (1989) Electrochemical and Surface Studies of Carbon Dioxide Reduction to Methane and Ethylene at Copper Electrodes in Aqueous Solutions. Journal of The Electrochemical Society 136: 1686.
14. Andrew A Peterson, Frank Abild-Pedersen, Felix Studt, Jan Rossmeisla, Jens K Nørskov (2010) How copper catalyzes the electroreduction of carbon dioxide into hydrocarbon fuels. Energy & Environment Science 3: 1311-1315.
15. Ki Dong Yang, Woo Ri Ko, Jun Ho Lee, Sung Jae Kim, Hyomin Lee, et al.(2017) Morphology-Directed Selective Production of Ethylene or Ethane from $CO_2$ on a Cu Mesopore Electrode. Angewandte international edition Chemie 56: 796–800.
16. Simelys Hernández, M Amin Farkhondehfale, Francesc Sastre, Michiel Makkee, Guido Saracco, et al. (2017) Syngas production from electrochemical reduction of $CO_2$: Current status and prospective implementation. Green Chemistry 19: 2326-2346.
17. Farkhondehfal MA, S Hernández, M Rattalino, M.Makkee, A Lamberti, et al. (2019) Syngas production by electrocatalytic

reduction of $CO_2$ using Ag-decorated $TiO_2$ nanotubes. International Journal of Hydrogen Energy 45: 26458-26471.
18. Hoffman ZB, Gray TS, Moraveck KB, Gunnoe TB, Zangari G (2017) Electrochemical Reduction of Carbon Dioxide to Syngas and Formate at Dendritic Copper-Indium Electrocatalysts. ACS Catalysis 7: 5381-5390.
19. T & Plan, YS 2014 Challenges and O Pportunities To Advance 2014: 1-28.
20. Le Duff CS, Lawrence M J, Rodriguez P (2017) Role of the Adsorbed Oxygen Species in the Selective Electrochemical Reduction of $CO_2$ to Alcohols and Carbonyls on Copper Electrodes. Angewandte international edition Chemie 56: 12919-12924.
21. Yoshio Hori, Akira Murata, Ryutaro Takahashi, Shin Suzuki (1988) ChemInform Abstract: Enhanced Formation of Ethylene and Alcohols at Ambient Temperature and Pressure in Electrochemical Reduction of Carbon Dioxide at a Copper Electrode. Journal of the Chemical Society, Chemical Communications 19: 17-19.
22. Raudaskoski R, Niemelä MV, Keiski RL (2007) The effect of ageing time on co-precipitated Cu/ZnO/$ZrO_2$ catalysts used in methanol synthesis from $CO_2$ and H2. Topics in Catalysis 45: 57-60.
23. Collins SE, Chiavassa DL, Bonivardi AL, Baltanás MA (2005) Hydrogen spillover in $Ga_2O3$-Pd/$SiO_2$ catalysts for methanol synthesis from $CO_2/H_2$. Catalysis Letters 103: 83-88.
24. Matsumura Y, Shen WJ, Ichihashi Y, Okumura M (2001) Low-temperature methanol synthesis catalyzed over ultrafine palladium particles supported on cerium oxide. Journal of Catalysis 197: 267-272.
25. Qian Q, Zhang J, Cui M, Han B (2016) Synthesis of acetic acid via methanol hydrocarboxylation with CO2 and $H_2$. Nature Communications 7: 1-7.
26. Gupta K, Bersani M, Darr J A (2016) Highly efficient electro-reduction of $CO_2$ to formic acid by nano-copper. Journal of Materials Chemistry A 4: 13786-13794.
27. Agarwal AS, Zhai Y, Hill D, Sridhar N (2011) The electrochemical reduction of carbon dioxide to formate/formic acid: Engineering and economic feasibility. Chemistry Sustainability energy mterials 4: 1301-1310.
28. Ik Seon Kwon, Tekalign Terfa Debela, In Hye Kwak, Hee Won Seo, Kidong Park, et al. (2019) Selective electrochemical reduction of carbon dioxide to formic acid using indium – zinc bimetallic nanocrystals. Journal of Materials Chemistry A 7: 22879-22883.
29. Ratnadip De, Sabrina Gonglach, Shounik Paul, Michael Haas, SS Sreejith, et al. (2020) Electrocatalytic Reduction of $CO_2$ to Acetic Acid by a Molecular Manganese Corrole Complex. Angewandte international edition Chemie 59: 10527-10534.
30. Premkumar J, Ramaraj R (1997) Photocatalytic reduction of carbon dioxide to formic acid at porphyrin and phthalocyanine adsorbed Nafion membranes. Journal of Photochemistry and Photobiology A: Chemistry 110: 53-58.
31. Kamphuis AJ, Picchioni F, Pescarmona PP (2019) $CO_2$-fixation into cyclic and polymeric carbonates: Principles and applications. Green Chemistry 21: 406-448.
32. Dunn AM, Hofmann OS, Waters B, Witchel E (2011) Cloaking malware with the trusted platform module. Proceedings of the 20th USENIX Security Symposium 2011: 395-410.
33. Zhang Q, Yuan HY, Fukaya N, Yasuda H, Choi JC (2017) Direct synthesis of carbamate from $CO_2$ using a task-specific ionic liquid catalyst. Green Chemistry 19: 5614-5624.
34. Indrakanti VP, Kubicki JD, Schobert HH (2009) Photoinduced activation of $CO_2$ on Ti-based heterogeneous catalysts: Current state, chemical physics-based insights and outlook. Energy&Environment Science 2: 745-758.
35. Freund HJ, Roberts MW (1996) Surface chemistry of carbon dioxide. Surface Science Reports 25: 225-273.
36. Xie S, Zhang Q, Liu G, Wang Y (2016) Photocatalytic and photoelectrocatalytic reduction of $CO_2$ using heterogeneous catalysts with controlled nanostructures. Chemical Communication 52: 35-59.
37. Bhupendra Kumar, Mark Llorente, Jesse Froehlich, Tram Dang, Aaron Sathrum, et al. (2012) Photochemical and Photoelectrochemical Reduction of $CO_2$. Annual Review of Physical Chemistry 63: 541-569.
38. Kondratenko EV, Mul G, Baltrusaitis J, Larrazábal GO. Pérez-Ramírez J (2013) Status and perspectives of $CO_2$ conversion into fuels and chemicals by catalytic, photocatalytic and electrocatalytic processes. Energy&Environment Science 6: 3112-3135.
39. Dhakshinamoorthy A, Navalon S, Corma A, Garcia H (2012) Photocatalytic $CO_2$ reduction by $TiO_2$ and related titanium containing solids. Energy&Environment Science 5: 9217-9233.
40. Yuan L, Xu YJ Photocatalytic conversion of $CO_2$ into value-added and renewable fuels. Applied Surface Science 342: 154-167.
41. Xiaojiang Zhang, Fei Han, Bo Shi, Samira Farsinezhad, Greg P Dechaine et al. Photocatalytic conversion of diluted $CO_2$ into light hydrocarbons using periodically modulated multiwalled nanotube arrays. Angewandte international edition Chemie 51: 12732-12735.
42. Recep Kas, Ruud Kortlever, Alexander Milbrat, Marc TM Koper, Guido Mul, et al. (2014) Electrochemical $CO_2$ reduction on Cu2O-derived copper nanoparticles: Controlling the catalytic selectivity of hydrocarbons. Physical Chemistry Chemical Physics 16: 12194-12201.
43. Yao Zheng, Anthony Vasileff, Xianlong Zhou, Yan Jiao, Mietek Jaroniec, et al. (2019) Understanding the Roadmap for Electrochemical Reduction of $CO_2$ to Multi-Carbon Oxygenates and Hydrocarbons on Copper-Based Catalysts. Journal of American Chemical Society 141: 7646-7659.
44. Albertus D Handoko, Kuang Wen Chan, Boon Siang Yeo (2017) -$CH_3$ Mediated Pathway for the Electroreduction of CO2 to Ethane and Ethanol on Thick Oxide-Derived Copper Catalysts at Low Overpotentials. ACS Energy Letters 2: 2103-2109.
45. Tsu-Chin Chou, Chiao-Chun Chang, Hung-Ling Yu, Wen-Yueh Yu, Chung-Li Dong, et al. (2020) Controlling the Oxidation State of the Cu Electrode and Reaction Intermediates for Electrochemical $CO_2$ Reduction to Ethylene. Journal of American Chemical Society 142: 2857-2867.
46. 46. Ruud Kortlever, Jing Shen, Klaas Jan P Schouten, Federico Calle Vallejo, Marc TM Koper (2015) Catalysts and Reaction Pathways for the Electrochemical Reduction of Carbon Dioxide. The Journal of Physical Chemistry Letters 6: 4073-4082.

47. Jinghua Wu, Yang Huang, Wen Ye, Yanguang Li (2017) $CO_2$ Reduction: From the Electrochemical to Photochemical Approach. Advanced Science 4: 1-29.
48. M Aulice Scibioh, Viswanathan (2004) Electrochemical Reduction of Carbon Dioxide: A Status Report. Indian National Science Academy 70: 407-462.
49. Zhao G, Huang X, Wang X, Wang X (2017) Progress in catalyst exploration for heterogeneous CO2 reduction and utilization: A critical review. Journal of Materials Chemistry A 5: 21625-21649.
50. Tackett BM, Gomez E, Chen JG (2019) Net reduction of $CO_2$ via its thermocatalytic and electrocatalytic transformation reactions in standard and hybrid processes. Nature. Catalysis 2: 381-386.
51. Al-Rowaili FN, Jamal A, Ba Shammakh MS, Rana AA( 2018) Review on Recent Advances for Electrochemical Reduction of Carbon Dioxide to Methanol Using Metal-Organic Framework (MOF) and Non-MOF Catalysts: Challenges and Future Prospects. ACS Sustainable Chemistry and Engineering 6: 15895-15914.
52. Jingxiang Low, Jiaguo Yu, Wingkei Ho (2015) Graphene-Based Photocatalysts for $CO_2$ Reduction to Solar Fuel. The Journal of Physical Chemistry Letters 6: 4244-4251.
53. Weilai Yu, Junxiang Chena, Tongtong Shang, Linfeng Chen, Lin Gu, et al. (2017) Direct Z-scheme g-C3N4/$WO_3$ photocatalyst with atomically defined junction for H2 production. Applied Catalysis B: Environmental 219: 693-704.
54. Tingmin Di, Bicheng Zhu, Bei Cheng, Jiaguo Yu, Jingsan Xu (2017) direct Z-scheme g-$C_3N_4$/$SnS_2$ photocatalyst with superior visible-light CO2 reduction performance. Journal of Catalysis 352: 532-541.
55. Habisreutinger SN, Schmidt Mende, Stolarczyk JK (2013) Photocatalytic reduction of $CO_2$ on $TiO_2$ and other semiconductors. Angewandte international edition Chemie 52: 7372-7408.
56. Jan Rongé, Tom Bosserez, David Martel, Carlo Nervi, Luca Boarino, et al. (2014) Monolithic cells for solar fuels. Chemical Society Reviews 43: 7963-7981.
57. Liu C, Dasgupta NP, Yang P (2014) Semiconductor nanowires for artificial photosynthesis. Chemistry of Materials 26: 415-422.
58. Shuying Zhu, Shijing Liang, Jinhong Bi, Minghua Liu, Limin Zhou, et al. (2016) Photocatalytic reduction of $CO_2$ with $H_2O$ to $CH_4$ over ultrathin SnNb2O6 2D nanosheets under visible light irradiation. Green Chemistry 18: 1355-1363.
59. David SA Simakov (2017) Thermocatalytic Conversion of CO2. Renewable Synthetic Fuels and Chemicals from Carbon Dioxide 2017:1-25.
60. Wang Z jun, Song H, Liu H, Ye J (2019) Coupling of Solar Energy and Thermal Energy for Carbon Dioxide Reduction: Status and Prospects. Angewandte international edition Chemie 59: 8016-8035.
61. Gerhard Ertl (2008) Reactions at surfaces: From atoms to complexity (nobel lecture). Angewandte international edition Chemie 47: 3524-3535.
62. Stefan Rönsch, Jens Schneider, Steffi Matthischke, Michael Schlüter, Manuel Götz, et al. (2016) Review on methanation - From fundamentals to current projects. Fuel 166: 276-296.
63. Hansen TW, Delariva AT, Challa SR, Datye AK (2013) Sintering of catalytic nanoparticles: Particle migration or ostwald ripening. Accounts of Chemical Research 46: 1720-1730.
64. Xianguang Meng, Tao Wang, Lequan Liu, Shuxin Ouyang, Peng Li, et al. (2014) Photothermal conversion of $CO_2$ into CH4 with H2 over Group VIII nanocatalysts: An alternative approach for solar fuel production. Angewandte international edition Chemie 53: 11478-11482.
65. Pengyan Li, Li Liu, Weijia An, Huan Wang, Hongxia Guo, et al. (2020) Ultrathin porous g-C3N4 nanosheets modified with AuCu alloy nanoparticles and C-C coupling photothermal catalytic reduction of CO2 to ethanol. Applied Catalysis B: Environmental 266: 118618.
66. Yufei Zhao, Wa Gao, Siwei Li, Gareth R Williams, Abdul Hanif Mahadi, et al. (2019) Solar- versus Thermal-Driven Catalysis for Energy Conversion. Joule 3: 920-937.
67. Ee Teng Kho, Tze Hao Tan, Emma Lovell, Roong Jien Wong, Jason Scott, et al. (2017) A review on photo-thermal catalytic conversion of carbon dioxide. Green Energy and Environment 2: 204-217.
68. Aslam U, Rao VG, Chavez S, Linic S (2018) Catalytic conversion of solar to chemical energy on plasmonic metal nanostructures. Nature Catalysis 1: 656-665.
69. Boerigter C, Campana R, Morabito M, Linic S (2016) Evidence and implications of direct charge excitation as the dominant mechanism in plasmon-mediated photocatalysis. Nature Communications 7: 1-9.
70. Yuchao Zhang, Shuai He, Wenxiao Guo, Yue Hu, Jiawei Huang, et al. (2018) Surface-Plasmon-Driven Hot Electron Photochemistry. Chemical Reviews 118: 2927-2954.
71. Manjavacas A, Liu JG, Kulkarni V, Nordlander P (2014) Plasmon-induced hot carriers in metallic nanoparticles. ACS Nano 8: 7630-7638.
72. Brown AM, Sundararaman R, Narang P, Goddard WA, Atwater HA (2016) Nonradiative plasmon decay and hot carrier dynamics: Effects of phonons, surfaces, and geometry. ACS Nano 10: 957-966.
73. Robatjazi H, Bahauddin SM, Doiron C, Thomann I (2015) Direct plasmon-driven photoelectrocatalysis. Nano letters 15: 6155-6161.
74. Christopher P, Xin H, Linic S (2011) Visible-light-enhanced catalytic oxidation reactions on plasmonic silver nanostructures. Nature Chemistry 3: 467-472.
75. Lunde PJ, Kester FL (1974) Carbon Dioxide Methanation on a Ruthenium Catalyst. Industrial and Engineering Process Design and Development 13: 27-33. (1974).
76. Wang W, Wang S, Ma X, Gong J (2011) Recent advances in catalytic hydrogenation of carbon dioxide. Chemical Society Reviews 40: 3703-3727.
77. Aziz, M. A. A., Jalil, A. A., Triwahyono, S. & Ahmad, A. $CO_2$ methanation over heterogeneous catalysts: Recent progress and future prospects. Green Chem. 17, 2647–2663 (2015).
78. Paul G O'Brien, Amit Sandhel, Thomas E Wood, Abdinoor A Jelle, Laura B, et al. (2014) Photomethanation of gaseous CO2 over ru/silicon nanowire catalysts with visible and near-infrared photons. Advanced Science 1: 1–7.
79. Jian Ren, Shuxin Ouyang, Hua Xu, Xianguang Meng, Tao Wang, et al. (2017) Targeting Activation of CO2 and $H_2$ over Ru-Loaded Ultrathin Layered Double Hydroxides to Achieve Efficient Photothermal $CO_2$ Methanation in Flow-Type Sys-

tem. Advanced Energy Materials 7: 1–7.
80. Liuliu Lin, Ke Wang, Kai Yang, Xun Chen, Xianzhi Fu, et al. (2017) The visible-light-assisted thermocatalytic methanation of CO2 over Ru/TiO(2-x)Nx. Applied Catalysis B: Environmental 204: 440-455.
81. Xiao Zhang, Xueqian Li, Du Zhang, Neil Qiang Su, Weitao Yang, et al. (2017) Product selectivity in plasmonic photocatalysis for carbon dioxide hydrogenation. Nature Communications 8: 1–9.
82. Low J, Zhang L, Zhu B, Liu Z, Yu J (2018) $TiO_2$ Photonic Crystals with Localized Surface Photothermal Effect and Enhanced Photocatalytic $CO_2$ Reduction Activity. ACS Sustainable Chemistry and Engineering 6: 15653-15661.
83. Yingying Li, Changhua Wang, Miao Song, Dongsheng Li, Xintong Zhang, et al. (2019) TiO2-X/CoOX photocatalyst sparkles in photothermocatalytic reduction of $CO_2$ with H2O steam. Applied Catalysis B: Environmental 243: 760-770.
84. Min Xu, Xiantao Hu, Shaolei Wang, Junchen Yu, Dajian Zhu, (2019) Photothermal effect promoting $CO_2$ conversion over composite photocatalyst with high graphene content. Journal of Catalysis 377: 652–661.
85. Xiaoding X, Moulijn JA (1996) Mitigation of $CO_2$ by chemical conversion: Plausible chemical reactions and promising products. Energy and Fuels 10: 305-325.
86. Jingyun Ye, Changjun Liu, Donghai Mei, QG (2013) Active Oxygen Vacancy Site for Methanol Synthesis from $CO_2$ Hydrogenation on In2O3(110): A DFT Study. ACS Catalysis 3: 1296-1306.
87. Porosoff MD, Yan B, Chen JG (2016) Catalytic reduction of $CO_2$ by H2 for synthesis of CO, methanol and hydrocarbons: Challenges and opportunities. Energy and Environmental Science 9: 62-73.
88. Erwin Lam, Kim Larmier, Shohei Tada, Patrick Wolf, Olga V Safonova, (2019) Zr(IV) surface sites determine CH3OH formation rate on Cu/ZrO2/$SiO_2$ - $CO_2$ hydrogenation catalysts. Chinese Journal of Catalysis 40: 1741-1748.
89. Waugh KC (1992) Methanol Synthesis. Catalysis Today 15: 51-75.
90. Jinghua Xu, Xiong Su, Xiaoyan Liu, Xiaoli Pan, Guangxian Pei, et al. (2016) Methanol synthesis from $CO_2$ and $H_2$ over Pd/ZnO/$Al_2O_3$: Catalyst structure dependence of methanol selectivity. Applied Catalysis A: General 514: 51-59.
91. Lu Wang, Mireille Ghoussoub, Hong Wang, Yue Shao, Wei Sun, et al. (2018) Photocatalytic Hydrogenation of Carbon Dioxide with High Selectivity to Methanol at Atmospheric Pressure. Joule 2: 1369-1381.
92. Dengdeng Wu, Kaixi Deng, Bing Hu, Qingye Lu, Guoliang Liu, et al. (2019) Plasmon-Assisted Photothermal Catalysis of Low-Pressure $CO_2$ Hydrogenation to Methanol over Pd/ZnO Catalyst. ChemCatChem 11, 1598–1601 (2019).
93. Zhen Hong He, Chong Shan Jiang, Kuan Wang, Zhong Yu-Wanga, Na Li, (2020) Photothermal $CO_2$ hydrogenation to methanol over a CoO/Co/$TiO_2$ catalyst in aqueous media under atmospheric pressure. Catalysis Today 356: 579-588.
94. Guangbo Chen, Rui Gao, Yufei Zhao, Zhenhua Li, Geoffrey IN Waterhouse, et al. (2018) Alumina-Supported CoFe Alloy Catalysts Derived from Layered-Double-Hydroxide Nanosheets for Efficient Photothermal $CO_2$ Hydrogenation to Hydrocarbons. Advanced Materials 30: 1-8.
95. Porosoff, M. D. & Chen, J. G. Molybdenum carbide as alternative catalysts to precious metals for highly selective reduction of $CO_2$ to CO. Catal. React. Eng. Div. 2014 - Core Program. Area 2014 AIChE Annu. Meet. 1, 578 (2014).
96. Chen CS, You JH, Lin CC (2011) Carbon nanofibers synthesized from carbon dioxide by catalytic hydrogenation on Ni-Na/Al2O3 catalysts. The Journal of Physical Chemistry 115: 1464-1473.
97. Vanessa M Lebarbier, Robert A Dagle, Libor Kovarik, Jair A Lizarazo Adarme, David L King, et al. (2012) Synthesis of methanol and dimethyl ether from syngas over Pd/ZnO/Al2O3 catalysts. Catalysis Science and Technology 2: 2116-2127.
98. Daza YA, Kuhn JN (2016) $CO_2$ conversion by reverse water gas shift catalysis: Comparison of catalysts, mechanisms and their consequences for $CO_2$ conversion to liquid fuels. RSC Advances 6: 49675-49691.
99. Centi G, Perathoner S (2009) Opportunities and prospects in the chemical recycling of carbon dioxide to fuels. Catalysis Today 148: 191-205.
100. Daza YA, Kent RA, Yung MM, Kuhn JN (2014) Carbon dioxide conversion by reverse water-gas shift chemical looping on perovskite-type oxides. Industrial and Engineering Chemistry research 53: 5828-5837.
101. Congjun Wang, Oshadha Ranasingha, Sittichai Natesakhawat, Paul R Ohodnicki, Mark Andio, et al. (2013) Visible light plasmonic heating of Au–ZnO for the catalytic reduction of $CO_2$. Nanoscale 5: 6968-6974.
102. Aniruddha A Upadhye, Insoo Ro, Xu Zeng, Hyung Ju Kim, Isabel Tejedor, et al. (2015) Plasmon-enhanced reverse water gas shift reaction over oxide supported Au catalysts. Catalysis Science and Technology 5: 2590-2601.
103. Hossein Robatjazi, Hangqi Zhao, Dayne F Swearer, Nathaniel J Hogan, Li Zhou, et al. (2017) Plasmon-induced selective carbon dioxide conversion on earth-abundant aluminum-cuprous oxide antenna-reactor nanoparticles. Nature Communications 8: 1-9.
104. Li Wang, Xinxin Liu, Yuanlin Dang, Haiquan Xie, Qiang Zhao, et al. (2019) Enhanced solar induced photo-thermal synergistic catalytic $CO_2$ conversion by photothermal material decorated TiO2. Solid State Sciences 89: 67-73.
105. Lu B, Quan F, Sun Z, Jia F, Zhang L (2019) Photothermal reverse-water-gas-shift over Au/$CeO_2$ with high yield and selectivity in $CO_2$ conversion. Catalysis Communications 129: 105724.